Forestry: An International Journal of Forest Research, 2025, **00**, 1–12
https://doi.org/10.1093/forestry/cpaf084
Original Article

Contributions of height allometry and within-species trait variation to uncertainty in estimates of tropical forest carbon stocks

Hannah Carle[1,*], Teresa Neeman[2], Helen Murphy[3], David Bauman[4,5,6], Oliver Binks[7], Ingrid Coughlin[8], Andrew Ford[3], Adrienne Nicotra[2], Patrick Meir[9]

[1]Hawkesbury Institute for the Environment, Western Sydney University, Bourke Street, Richmond NSW 2753, Australia
[2]Research School of Biology, Australian National University, 134 Linnaeus Way, Acton ACT 2601, Australia
[3]Commonwealth Scientific and Industrial Research Organisation (CSIRO), TBuilding 145, James Cook University, James Cook Drive, Townsville, QLD 4811, Australia
[4]AMAP, University Montpellier, CIRAD, CNRS, INRAE, IRD, Montpellier, 2196 Bd de la Lironde, 34980 Montferrier-sur-Lez, France
[5]Environmental Change Institute, School of Geography and the Environment, University of Oxford, S Parks Rd, Oxford OX1 3QY, UK
[6]Laboratoire d'écologie Végétale et Biogéochimie, Université Libre de Bruxelles, Campus Plaine, Bâtiment BC (5th Floor, Wing C), Boulevard du Triomphe, CP 244, 1050 Brussels, Belgium
[7]CREAF (Centro de Investigación Ecológica y Aplicaciones Forestales), Campus UAB, Edifici C, 08193 Bellaterra (Cerdanyola del Vallès), Barcelona, Spain
[8]Australian Plant Phenomics Network, School of Agriculture, Food and Wine, University of Adelaide, Building WT81, Hartley Grove, Urrbrae SA 5064, Australia
[9]School of Geosciences, University of Edinburgh, Crew Building, King's Buildings West Mains Road, EH9 3JW Edinburgh, United Kingdom
*Corresponding author. Hawkesbury Institute for the Environment, Western Sydney University, Richmond, NSW, Australia. E-mail: H.Carle@westernsydney.edu.au

Abstract

Tropical forests host globally significant carbon stocks, which are relied on to help mitigate the effects of human-induced climate change. Characterizing the uncertainty around carbon stock estimates is thus essential to inform the carbon budgets needed to safely limit global warming, with implications for policy and decision-making worldwide. We used a large forest inventory dataset from the Australian tropical rainforest (7208 stems) to evaluate height:diameter (H:DBH) allometric variation and quantified within-species variation in wood density (WD) and woody tissue carbon ([C]) content (98 trees). Together, H:DBH, wood density, and woody tissue C were used to estimate forest carbon stocks (i.e. the carbon content of woody biomass: C_{AGB}). Using simulations, we then provide estimates and recommendations on the uncertainty around C_{AGB}. H measurement errors contributed more random error (4.5%) to C_{AGB} than the best performing (site-level) H:DBH allometric models (±2.4%) and led to under-estimation of C_{AGB} by roughly 15%. Comparison of H:DBH allometric models that were developed at different biogeographic scales shows that widely used pantropical models substantially over-estimated tree H, and thus tropical forest C_{AGB}, at some Australian sites by close to 100%. By contrast, wood trait variation generated just 3% uncertainty in C_{AGB}, which is reassuring since global wood trait datasets often contain a single record or a few records for tropical species. Our findings reinforce the promise of laser scanning technologies to improve biomass estimation via more accurate measurements of canopy height and nondestructive development of local-to-regional allometric models, which provide clear advantage over pantropical equations.

Keywords: height allometry; intraspecific variation; carbon stock; uncertainty; natural assets; LTER

Introduction

Accurately quantifying forest carbon underpins our capacity to make and enforce accurate carbon budgets and to ensure cost-effective and trustworthy investments in natural capital. Tropical forests have the potential to deliver substantial climate change mitigation (Griscom et al. 2017, Walker et al. 2022); they have absorbed large quantities of human carbon dioxide emissions to date and represent vast carbon stocks (Pan et al. 2011, Phillips et al. 2017, Pan et al. 2024). However, the total magnitude of carbon stocks and fluxes for tropical forests remains highly uncertain (Pan et al. 2024), which limits the capacity of governments, industries, and ecology practitioners to assess or manage climate change (Brienen et al. 2015, Hubau et al. 2020, Bauman et al. 2022) and land use threats (Malhi and Phillips 2004, Murphy and Romanuk 2014), or to fully leverage opportunities via natural capital. Largely, these uncertainties arise from the current methodologies used to estimate carbon.

Aboveground woody biomass (AGB, Mg) is generally estimated using allometric equations that are empirically derived from tree harvest data, collated at broad geographic scales (Chave et al. 2005, Feldpausch et al. 2012, Chave et al. 2014). These allometric equations rely on some or all of the following variables: tree height (H, m) (Feldpausch et al. 2012), tree diameter—most often diameter at breast height (DBH, cm)—and wood density (WD, g cm^{-3}). The initial calculation of tree volume is a function of DBH and H, where height is sometimes measured but often estimated from DBH in one of several ways. AGB is a function of tree volume multiplied by WD [Equation (1), Chave et al. (2014)], which is then multiplied by the percentage carbon content in woody tissue ([C])

Handling editor: Dr. Mark Ducey
Received 25 March 2025; **revised** 21 August 2025; **accepted** 13 November 2025

(Thomas and Martin 2012, Martin et al. 2018) to give an estimate of carbon in AGB (C_{AGB}).

Biases arising from AGB allometric equations, including in relation to tree-size and sample-size error-dependency, have been dealt with elsewhere (Chave et al. 2004, Hunter et al. 2013, Molto et al. 2013, Ledo et al. 2016). Here, we focus on biases associated with the constituent components of AGB models, which vary across landscapes (Chave et al. 2004, Roxburgh et al. 2015) and with ontogeny (Falster et al. 2018, Rodriguez-Zaccaro et al. 2019). Of these AGB components, DBH is usually measured for all trees, *H* is sometimes measured for a subset of trees, and WD is usually sourced from databases of species-, family-, or genus-level values compiled from the literature. Sometimes, one or more of these variables is not measured or is unavailable due to limited budgetary resources or other logistic constraints. When these variables are not measured, they must be somehow approximated (based on equations or known or expected distributions), and these approximations can generate systematic and random errors in forest carbon estimates. The uncertainties associated with such approximations should thus be carefully considered and reported, based on knowledge of the magnitude and drivers of variation in each parameter.

Tree *H* is particularly difficult to measure due to canopy density and complexity in tropical forests (Larjavaara et al. 2013) and is often estimated from DBH, based on the allometric relationship between *H* and DBH (*H*:DBH). The form of *H*:DBH is a nondecreasing curve that may or may not be asymptotically bounded (Ledo et al. 2016). Missing *H* values can be estimated using published allometric models or models derived from *H* and DBH measurements at a given study site (or collection of sites), and choice of the *H*:DBH equation is integral to the accuracy and precision of biomass estimates (Chave et al. 2005, Feldpausch et al. 2012, Molto et al. 2013). *H*:DBH allometry varies across scales, however, due to environmental, ecological, and phylogenetic factors (Feldpausch et al. 2011, Banin et al. 2012, Ibanez et al. 2018, Jucker et al. 2022). Trees in drier climates or in stands with higher basal area, for example, tend to be shorter at a given DBH (Feldpausch et al. 2011, Binks et al. 2023). While it might be expected that *H*:DBH models defined at smaller spatial scales—continent, region, or stand—would consistently outperform more widely applicable pantropical models, the evidence for this is mixed (Banin et al. 2012, Feldpausch et al. 2012, Ledo et al. 2016). Particularly in forest types with high species diversity, and in situations where the scale and extent of *H*:DBH variation is not well characterized, the potential benefits of using smaller-scale allometric equations may be counteracted by sample size and representativity issues, resulting in poor out-of-sample predictions (Chave et al. 2004, Hunter et al. 2013).

There is additional uncertainty in C_{AGB} because of measurement errors in DBH and *H*. DBH measurement errors (ε_{DBH}) are generally small in magnitude and have been well characterized by repeat measurements (Condit et al. 2004); nonetheless, these errors do scale to C_{AGB}. Conversely, *H* measurement errors (ε_{Hmeas}) tend to be highly variable and biased (whether from laser rangefinder or clinometer and tape measure methods) (Hunter et al. 2013, Larjavaara et al. 2013). Use of Light Detection And Ranging (LiDAR) laser scanning (LS) methods to measure tree *H* and AGB is expanding. This method estimates the geometry of target objects by emitting laser pulses from a scanner and recording the response time of reflections from the target. Expanding use of LS methods will undoubtedly improve measurement-related uncertainties in C_{AGB}—particularly for large trees, since *H* measurement error and allometric error typically increase with tree size (Calders et al. 2014, Disney 2019, Burt et al. 2020, Terryn et al. 2024). A recent pantropical evaluation of the *H* measurement bias associated with traditional inventory methods [cross-validated using terrestrial laser scanning (TLS)] suggests it is −5.3% to −25.4% (for 30 m trees), ranging up to −41.3% for very tall tropical trees (77 m dipterocarps) (Terryn et al. 2024). Despite increasing performance advantages to LS over traditional allometric approaches (e.g. Terryn et al. 2024), the advantages are likely dependent on forest type, and LS remains challenging to deploy in remote locations and is technically demanding in terms of postprocessing (Lines et al. 2022). Thus, many contend that traditional inventory methods are likely to continue in broad use for years to come—all at a time when carbon markets are developing at an unprecedented pace, and the need for accurate accounting of ecosystem carbon is greater than ever.

The next component of C_{AGB} estimation is WD. Inclusion of WD in AGB allometric models is thought to reduce uncertainty in estimates of AGB even more than inclusion of tree *H* (Chave et al. 2005). WD varies among species and species turnover substantially influences stand-level biomass (Baker et al. 2004, Phillips et al. 2019). Genus-level data are commonly used if species-level data are unavailable. WD also varies within species—across environmental gradients (Patiño et al. 2009) and with tree size (Phillips et al. 2019). The magnitude of within-species WD variation is not well characterized, although one assessment of 50 Neotropical tree species, which had more than six measurements available (Chave et al. 2004), suggested a within-species standard deviation (SD) of 10%. Using a pantropical mean for WD in place of species-specific WD values results in a 15% over-estimate of global carbon stocks in tropical forests (Baker et al. 2004, Phillips et al. 2019). Not accounting for within-species WD variation can bias estimates of AGB (Molto et al. 2013). There is hence a clear need to better evaluate WD variation and the extent to which it scales to estimates of C_{AGB}.

The influence of [C] variation on C_{AGB} estimation has received comparatively little attention. [C] in trees increases with WD and generally increases with tree diameter (Ma et al. 2020) but may also vary across landscapes via environmental influences on growth and WD (Elias and Potvin 2003, Martin et al. 2018, Ma et al. 2020). While the magnitude of [C] differences is typically small (between 0.40 and 0.50 for tropical angiosperm species) (Thomas and Martin 2012, Martin et al. 2018), the effect of [C] on C_{AGB} is multiplicative, so small inaccuracies may scale to large differences in C_{AGB} (Elias and Potvin 2003, Martin et al. 2018). An important first step has been to develop robust estimates of mean [C] for different biomes (Thomas and Martin 2012, Martin et al. 2018). Assuming that 50% of AGB was [C] (instead of using a tropical mean derived from data) led to over-estimates of global tropical forest carbon stocks by 20.1 Pg C or 8.9% (Martin et al. 2018).

Here, we assess uncertainties around C_{AGB} for Australian moist tropical forests that arise from site-to-site variation in *H*:DBH and within-species variation in WD and [C]. We compare the magnitude of these uncertainties with those arising from *H* and DBH measurement errors and *H*:DBH allometric model choice (comparing models derived at different biogeographic scales). To do this, we used extensive forest inventory records (*H* and DBH measurements) from 20 sites in the Queensland Permanent Rainforest Plots–Commonwealth Scientific and Industrial Research Organisation (QPRP-CSIRO) network and measured WD and [C] for 255 wood cores from seven common species. These data are used to simulate C_{AGB} and quantify the uncertainties associated

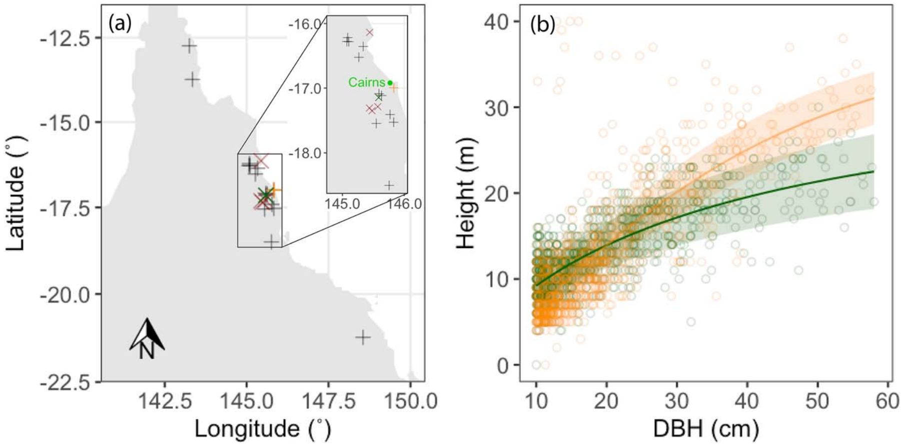

Figure 1. (a) Site locations of the 20 plots in Queensland, Australia, and (b) an example of height-diameter (H:DBH) allometry in two plots. (a) '×' indicates locations where wood cores were sampled. (b) Weibull functions fit to H and DBH measurements from different sites illustrate divergent allometries; EP37 Eungella (orange, upper line) and EP29 Mount Fisher (green, low line) differ in elevation (920 and 1200 m, respectively), stem density (246 and 438 stems at last census: Table S1) and maximum stem diameter (156.6 and 93.4 cm).

with each variable. Based on these analyses, we make recommendations about measurement, sampling, and allometric model practices relevant to forest carbon practitioners globally.

Materials and methods

Site data

The QPRP network includes 20 0.5 ha (100 × 50 m) plots that were established by the CSIRO between 1971 and 1982 (Bradford et al. 2014) (now QPRP-CSIROplots). The plots capture much of the biogeographical diversity of Australian tropical forests (Fig. 1), with mean annual rainfall ranges from 1200 to 7000 mm and mean annual temperature ranges from 16°C to 26°C (see Table S1 for details).

In these plots, stems ≥10 cm DBH were resurveyed every 2–15 years (mean 3.17 ± 1.73 years, median 2.12), and mortality or physical damage was recorded. Tree height was measured at the time when plots were established and again in 1998. When each plot was established, researchers estimated tree heights, validated against canopy measurements using the triangulation method with a clinometer and measuring tapes (Graham et al. 2006). In 1998, tree H was measured using either the triangulation method or a laser rangefinder (Bushnell, Kansas, US) (Graham et al. 2006). All stems have been identified to the species level. The resulting dataset includes records for 10 701 trees over the 49-year observation window.

Variation in wood density and carbon content

We collected 255 wood microcores (Trephor Microcorer, CMC, Italy) from 98 trees belonging to seven common species across the plot network (Table 1). Focal species were selected on the basis of abundance (minimum two individuals at three plots per species) across plots with contrasting altitude and/or latitude. We attempted to sample trees that represented a wide range of DBH size classes for each species at each site. The microcore samples were collected opportunistically during a field campaign in June 2022 and so are geographically restricted to plots within 200 km of the towns of Cairns and Atherton.

For each tree, we cut bark windows roughly 15 cm below DBH at three points around the circumference of the tree, and sampled microcores (2 × 15 mm) from each window, resulting in 255 samples from 98 stems. Wood cores were stored in small humidified Eppendorfs and processed within 24 h. We estimated the dimensional volume of the fresh wood cores (Chave 2005), using length measured to the closest 0.5 mm and the internal diameter of the Trephor microcore. We stored the cores in vials with silicon beads and dried them for 3 days in a 70°C oven before measuring their dry mass. We estimated WD by dividing dry mass by volume (g cm^{-3}).

To assess [C] and WD, wood cores were prepared for mass spectrometry by grinding the entire core to homogenize across growth rings. Approximately 1 mg of ground material was analysed for carbon bulk content using an Elementar Isoprime CF-IRMS (Continuous-flow Isotope Ratio Mass Spectrometer). Carbon measurements were calibrated against standards of C_3 Beet sucrose (Beet87) and a C_4 cane (ANU) sucrose and are reported as percentage mass.

We estimated within-species variation in WD and [C] using the coefficient of variation (CV = standard deviation divided by the mean). We evaluated the sources of variation in stem-level WD and [C] using simple (linear) regression models parameterized by tree DBH, species, and site, with two-way interactions to enable species wood traits to vary differently across sites and tree sizes (i.e. WD ∼ DBH × species + site × species). We partitioned variance from these linear models to each fixed effect by estimating the R^2 of each factor or interaction (sum of squares for each factor divided by the total sum of squares for all model factors). We further tested for an expected positive association between [C] and WD (Martin et al. 2018) at the interspecies level ([C] ∼ WD) and within species ([C] ∼ WD + (1|species): package '*lmerTest*' (Kuznetsova et al. 2017)). These models and all following analyses were done in R version 4.5.0 (R Core Team 2025).

Estimating tree height

Tree heights are commonly estimated from DBH data by fitting a function to available height and diameter measurements of a species or forest stand. We created a randomized 50–50 (training-test) split of the available height data, stratified by measurement year and tree size. We derived site-level (20 sites, models fit to each site) and regional (all 20 sites together) H:DBH allometric models from the training dataset using function 'nls' in package '*car*' (Fox and Weisberg 2019) to fit Weibull three-parameter functions (Ledo et al. 2016) and extracted the coefficients a, b, and k of these

Table 1. Wood core sampling for seven common species in the QPRP network. Sampling of wood microcores was done during a 2022 field campaign, for a minimum of three sites per species (n_{site}) and minimum of nine samples per species (n_{stem}). We attempted to capture a representative range of DBH for each species at each site (min and max DBH).

Species	Code	n_{site}	n_{stem}	Mean n_{stem}/site	Min. DBH (cm)	Max. DBH (cm)
Aleurites rockinghamensis	*Ar*	3	13	4	14.6	91.0
Antirhea tenuiflora	*At*	3	11	4	11.1	25.4
Endiandra monothyra subsp. *monothyra*	*Emm*	4	10	2	10.7	31.1
Flindersia brayleyana	*Fb*	3	13	4	14.1	124.3
Franciscodendron laurifolium	*Fl*	3	28	9	10.1	72.7
Litsea leefeana	*Ll*	3	14	5	15.4	57.0
Xanthophyllum octandrum	*Xo*	3	9	3	13.0	50.7

models:

$$H = a \times \left(1 - \exp\left(-b \times \left(\mathrm{DBH}^{k}\right)\right)\right) \tag{1}$$

We then evaluated the performance of these *H*:DBH allometric models alongside three widely used *H*:DBH models from the literature (also Weibull three-parameter functions) using the test dataset. These additional models included one Australian and two pantropical functions (Feldpausch et al. 2012), with one of the pantropical functions additionally parameterized by environmental stress (*E*) (Chave et al. 2014). This parameter *E* combines temperature seasonality (TS), precipitation seasonality (PS), and maximum climatological water deficit (MCWD) to approximate major biogeographic differences across latitudes and elevations (Chave et al. 2014). To calculate *E*, monthly climate data were extracted from ANUClimate v.2.0 (0.01° grid) (Hutchinson et al. 2022). TS and PS were calculated as the standard deviation of monthly mean temperature (°C) and monthly rainfall (mm), expressed as a percentage of the mean (multiplied by 100). Monthly maximum climatological water deficit (MCWD) was calculated by identifying the most extreme monthly CWD in the previous 12-month period, where CWD is a measure of cumulative water deficit based on rainfall and actual evapotranspiration (Aragão et al. 2007, Malhi et al. 2009). MCWD was reset to zero at the wettest month of the year, based on 30-year (1981–2010) mean monthly precipitation values and given an upper bound of 1000 mm deficit. We calculated *E* for each plot at each census using the 6 months of data before and after each census date ($n = 256$). These census-level values for *E* were then averaged (across censuses) for each plot.

Estimating aboveground biomass

Aboveground biomass (AGB) was modelled using the Chave et al. (2005) moist forest equation. We preferred this equation over more recently published equations in Chave et al. (2014) because their performance is comparable and we preferred an equation defined using moist forest data only over the alternative, which used moist, dry, and wet forest data.

Tree *H* for calculation of AGB was taken from five different *H*:DBH allometric models: one site-level model, one regional model, and three models from the literature. WD (g cm^{-3}) data collated from literature and field collections (Bradford and Murphy 2019) was used to calculate the mean WD for each species (note that this database does not indicate whether the same or multiple methods were used to derive WD, which may introduce additional variation).

We used heartwood measurements where available (426 species) or otherwise combined heartwood and crosswood measurements (36 species). Where species-level values were not available, we averaged available heartwood data at the genus level (12 species) or for all available heartwood samples (3 species). We note that the median number of samples per species is $n = 1$. The biomass of strangler figs ($n = 59$) was calculated based on measurements or estimates of DBH of all stem segments combined. Palms, cycads, and lianas were excluded from all analyses.

Assessing height:diameter model choice

We first evaluated whether *H*:DBH allometric variation results in distinct allometries among sites. We fit two *H*:DBH allometric models to data for trees with DBH within a size range common to all plots (10.0–58.3 cm DBH)—one with unique parameter estimates for each plot and one without. These were fit using the 'nls' function in the R package '*car*' and were compared using analysis of variance and AIC.

We then assessed the relative performance of a suite of five *H*:DBH allometric model sets (one set of 20 site-level models, 1 regional model, and 3 models from the literature) in reference to measurements of *H* (H_{meas}). To do this, we quantified tree-level H_{mod} error by calculating mean error (ME, metres) as the sum of individual errors ($H_{mod} - H_{meas}$) divided by the number of trees, symmetric signed percentage bias (SSPB, %), and median symmetric accuracy (MSA, %) (Morley et al. 2018). We also compared percentage bias and uncertainty for AGB estimates (as derived from H_{mod} versus H_{meas}) aggregated at the plot level, using ME and root mean squared error (RMSE), normalized to AGB. We also quantified errors in each 10 cm diameter size class (trees >100 cm DBH were grouped together due to lower numbers of individuals) using ME of AGB for trees in each 10 cm DBH size class in each plot, normalized to AGB in that sample.

Simulations of uncertainty in AGB

We simulated uncertainty in AGB estimates given five scenarios: (i) no information about uncertainty; (ii) information on measurement precision and bias for *H* and DBH; (iii) within-species variation in WD and/or [C]; (iv) *H*:DBH allometric model uncertainty; and (v) information for (ii–iv) together. Given each information scenario, we ran 1000 simulations based on all trees alive at the last census (7208 stems). For each tree, DBH measurements, database WD values, and modelled heights were used as the basis

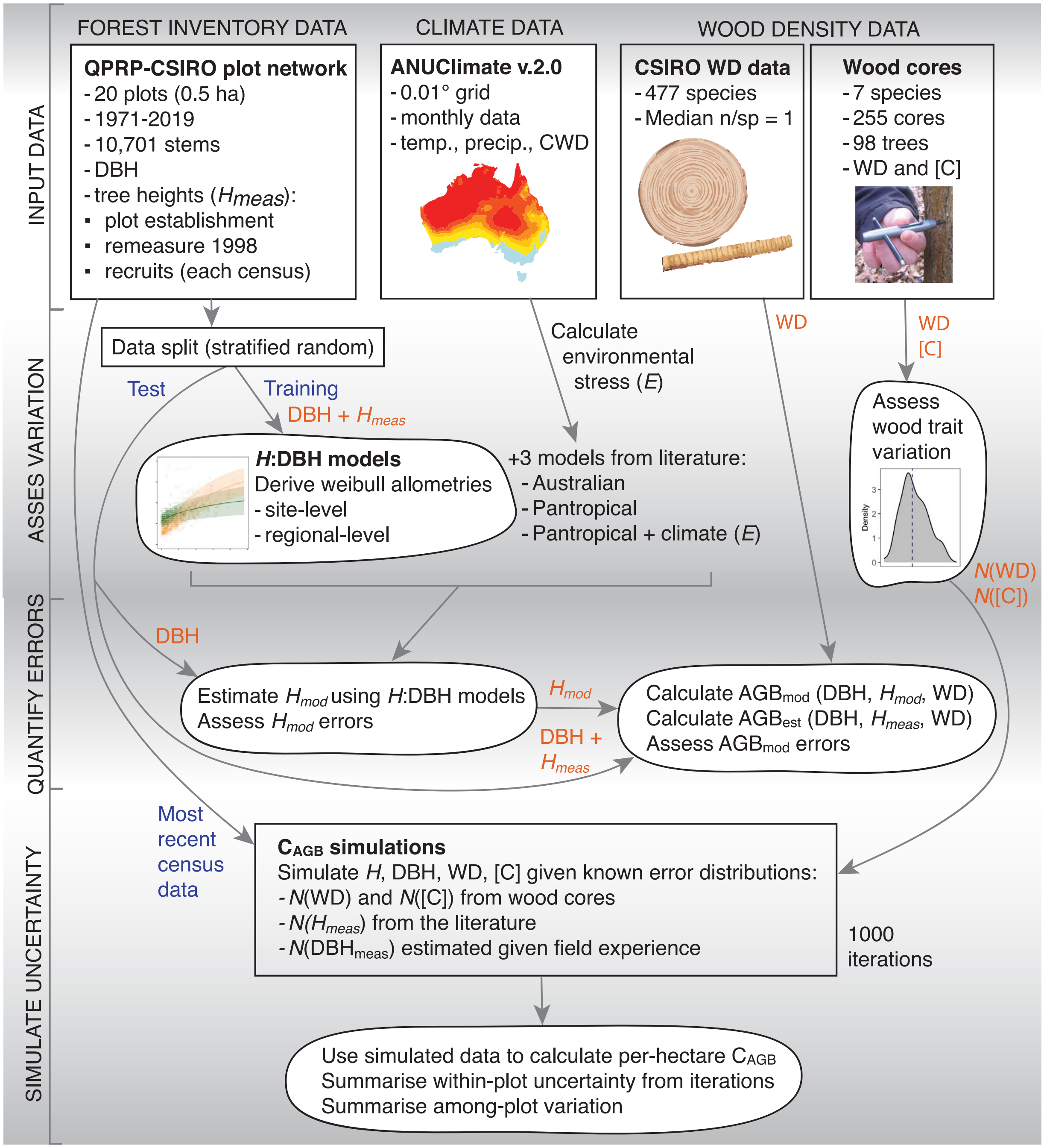

Figure 2. Overview of data sources, workflow, and how parameters (red text) were derived and utilized in subsequent models and simulations. Climate data included temperature (temp.), precipitation (precip.), and climatological water deficit (CWD) (see Methods for details).

for a simulated tree, for which simulated values of each variable were randomly sampled from normal distributions adjusted for bias and uncertainty (as standard deviations). These simulated tree measurements were then used to calculate plot-level (0.5 ha) C_{AGB}, resulting in 1000 C_{AGB} estimates per plot. These were multiplied by two to convert to per-hectare estimates. Means and standard deviations (SD) of simulated C_{AGB} estimates were used to summarize within-site uncertainty, while means and standard errors (se) were used to summarize among-plot variability. Below, we detail how information on precision and bias was incorporated in these simulations.

Characterising H_{meas} errors at our remote field sites would require resource-intensive canopy access and was beyond the scope of the present study. Instead, we approximated H_{meas} error distributions (ε_{Hmeas}) based on two prior studies (Hunter et al. 2013, Larjavaara et al. 2013) and simulated height measurement errors using $\varepsilon_{Hmeas} \sim N(H_{meas} - 2.1, 6.8\text{ m})$. DBH measurement errors were approximated with distribution $\varepsilon_{DBHmeas} \sim N(DBH_{meas}, 0.25\text{ cm})$ based on experience of repeat measurements by our team.

For WD, we simulated from normal distribution $\varepsilon_{WD} \sim N(\mu_{WD}, \sigma_{WD})$, where μ_{WD} was species mean WD and σ_{WD} was the average standard deviation for species WD, as calculated from the database described above (Bradford and Murphy 2019). For [C], we simulated from distribution $\varepsilon_{[C]} \sim N(0.465, \sigma_{[C]})$, where 0.465 is the current best estimate of [C] for tropical angiosperms

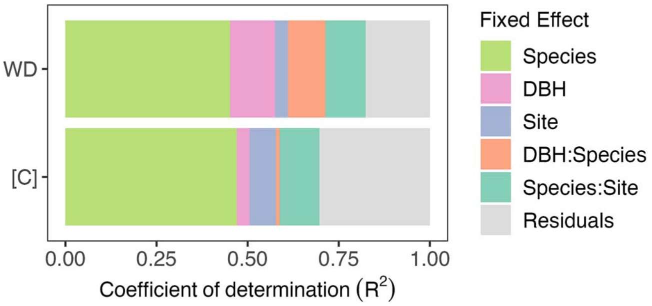

Figure 3. Sources of variation in wood density (WD) and woody tissue carbon content ([C]) for seven species at five sites. Variance was partitioned from linear models with fixed effects for species, tree diameter (DBH), site, and select interactions. The 'species:site' interaction accounts for intraspecific variability among sites, the 'site' fixed effect is the average site effect across species present at each site and reflects differing species assemblages. Model residuals are shaded grey.

(Martin et al. 2018) and $\sigma_{[C]}$ was the average standard deviation for species-level [C].

H:DBH model errors were simulated using a truncated normal distribution: $\varepsilon_{\text{est}} \sim \text{N}(H_{\text{mod}} + \text{model bias, RMSE})$, where plot-level RMSE was used to approximate a standard deviation. Tree height simulations were truncated such that H was between 5 m and the maximum measured H in the forest + 5 m. For simulation scenario (5), which combined H_{meas} and height allometric model uncertainties, we added normally distributed errors from H_{meas} and H_{mod} before applying the truncation.

Results

Variation in wood density and carbon content

Roughly half of stem-level variation in WD and [C] was captured by species differences (Fig. 3). Beyond species, both traits varied significantly in relation to DBH, and wood trait variation with DBH and among sites was dependent on species (Table S2). The dependency of [C] on WD showed that [C] correlated with WD at the interspecies level (ANOVA: $F = 8.55_{(1,252)}$, $P = .004$, model $R^2 = 0.292$) but not for individuals within a species (i.e. a linear mixed effects model with species as a random effect: $P = .747$, model $R^2 = 0.033$).

The coefficient of variation (CV) for WD ranged between 5% and 14% within species (7 species, $n = 9$–28 stems per species: Table 1) and between 5% and 9% within sites (across up to five focal species within each site) (Fig. 2). The magnitude of WD variation was similar when calculated from average species wood density values (i.e. species WD means only, SD = 0.09, $n = 7$) versus from all intraspecific wood density values pooled together (i.e. including intraspecific variation, SD = 0.11, $n = 255$). The coefficient of variation (CV) for [C] ranged between 21% and 62% within species and 16% and 57% within sites (across species within each site). Mean [C] (46.1 ± 1.6%; SD) calculated from all 254 wood samples was comparable to the pantropical mean for angiosperms (Fig. 2b; 45.6 ± 0.2%: Martin et al. (2018)), however, estimates of [C] from WD using the best available equation (Martin et al. 2018) tended to over-estimate [C] by 0.8% mass (−0.6% to 2.5%) at species level and by −8.3% to 12.4% in individual samples.

Assessing height:diameter model choice

The 20 QPRP-CSIRO plots differed substantially in H:DBH allometry based on H_{meas} and DBH$_{\text{meas}}$ errors (Table S3). The H:DBH allometric model stratified by site was significantly better than the unstratified, regional model (ANOVA: $F = 19.018_{(57,\,18425)}$, $P < .001$). Site-level empirical H:DBH models minimized both random error and systematic bias in H_{mod}, while our regional empirical model generated slightly more uncertainty (Table 2, Fig. 5). Models derived at larger biogeographic scales consistently resulted in over-estimates of plot-level AGB. The Australia-region H:DBH model (Feldpausch et al. 2012) demonstrated a mean individual H_{mod} bias of 12.5% (+1.5 m), which scaled to a mean plot-level AGB bias of 7.7%. One pantropical H:DBH model (Feldpausch et al. 2012) generated a mean individual H_{mod} bias of 17.2% (+2.3 m) and a mean plot-level AGB bias of 16.9%; the second pantropical H:DBH model (Chave et al. 2014) generated a mean individual H_{mod} bias of 71.0% (10.5 m) and a mean plot-level AGB bias of 66.6% respectively (Table 2), with mean plot-level AGB bias ranging from 25.8 to 101.1% among plots. Precision in plot-level AGB (percentage errors) generally declined for larger size classes (Fig. 5).

Simulations of uncertainty in forest carbon

The magnitude of mean uncertainty around per-hectare C_{AGB} (standard deviation of plot-level C_{AGB} normalised to regional mean C_{AGB}) ranged from 1.9% to 5%, depending on the choice of the H:DBH allometric model (Table S4). Biases in C_{AGB} increased with the scale at which the H:DBH model was defined (Fig. 5a, Table 2, Table S4), being greatest for the Chave et al. (2014) pantropical H:DBH model (mean plot-level bias 34.1%) (Table S4).

The magnitude of mean uncertainty around per-hectare C_{AGB} arising from measurement errors was as follows: ±0.2% from DBH$_{\text{meas}}$ (0.3 Mg C ha^{-1}); ±4.8% from H_{meas} (11.1 Mg C ha^{-1}); and 4.4% from DBH$_{\text{meas}}$ and H_{meas} errors combined (10.3 Mg C ha^{-1}). The magnitude of uncertainty around per-hectare C_{AGB} arising from within-species variation in WD and [C] was small: ±3.2% (6.8 Mg C ha^{-1}) and ±0.7% (1.5 Mg C ha^{-1}), respectively (Fig. 5b, Table S4).

Given information on H_{meas}, DBH$_{\text{meas}}$, WD, and [C] variation, as well as uncertainty associated with the best-performing (site-level) H:DBH model, resulting uncertainty around per-hectare C_{AGB} was ±4.5% or 10.4 Mg C ha^{-1} (Fig. 5b: Table S4). Under any of the information scenarios, C_{AGB} varied by 26%–32% among plots (Table S4).

Discussion

We assessed the uncertainty around mean per-hectare C_{AGB} given allometric and within-species wood trait variation for 20 floristically and structurally diverse plots in Australian moist tropical rainforest (Fig. 1a). The choice of the H:DBH allometric model generated the largest uncertainty around forest carbon estimates, with site-level models performing notably better than pantropical ones. Height measurement errors contributed most uncertainty to per-hectare C_{AGB} (4.9% within-plot SD: Table S4), whereas diameter measurement error had a negligible effect (0.1%). Within-species variation in wood density contributed substantially more uncertainty (1.7%) to C_{AGB} than within-species variation in [C] (0.7%). Given information on all these sources of uncertainty together, and assuming the use of site-level H:DBH models, the average random error on per-hectare C_{AGB} was 6.4% while the mean bias across plots was 9.8% (Table S4).

Allometric and within-species trait variation thus appear to contribute considerably less uncertainty to C_{AGB} than that associated with either AGB allometric models (10%–20%: Keller et al. 2001, Chave et al. 2004, Molto et al. 2013) or sampling issues

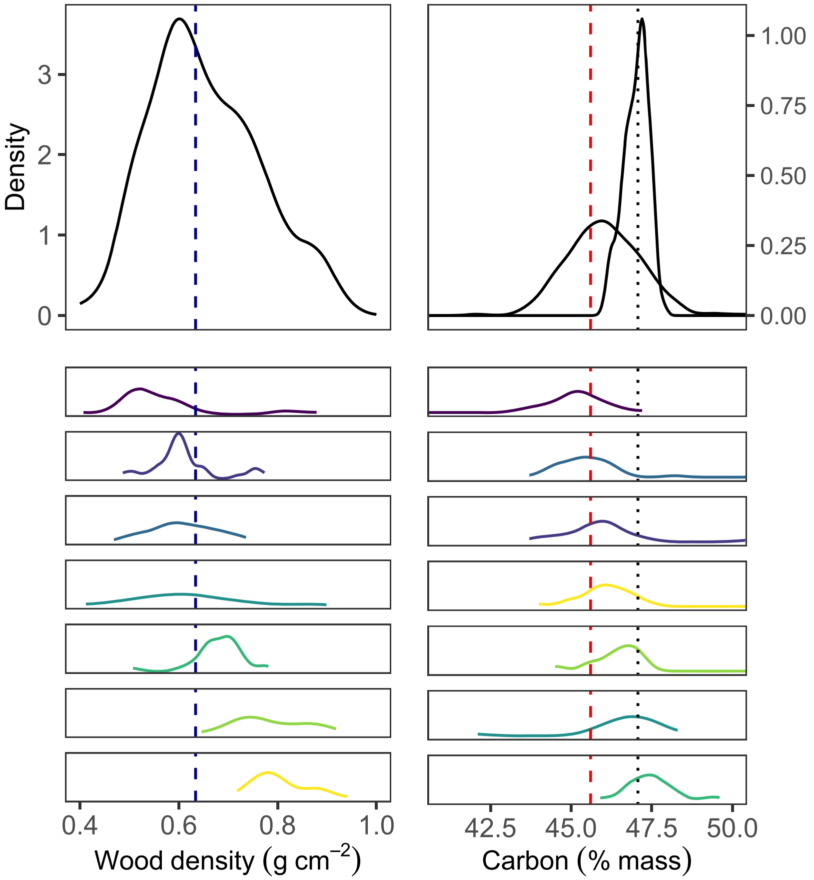

Figure 4. Wood density (LHS) and woody tissue carbon content (RHS) across species (top panels, in dark grey: *n* = 255 wood cores, 98 stems, 5 sites) and within-species (see Table 1 for species names, codes, sample sizes). Species are represented by the same colours for wood density and carbon content. LHS: dashed blue line indicates median wood density for all tree species in the QPRP-CSIRO plot network (unpublished data, CSIRO, *n* = 770 samples, 460 tree species). RHS: dashed red line indicates the current best estimate of mean [C] for tropical angiosperms (Martin et al. 2018). RHS: light-grey density distribution (dotted line marked at median for visual aid) depicts estimates of [C] derived from our WD measurements using a global regression equation (Martin et al. 2018).

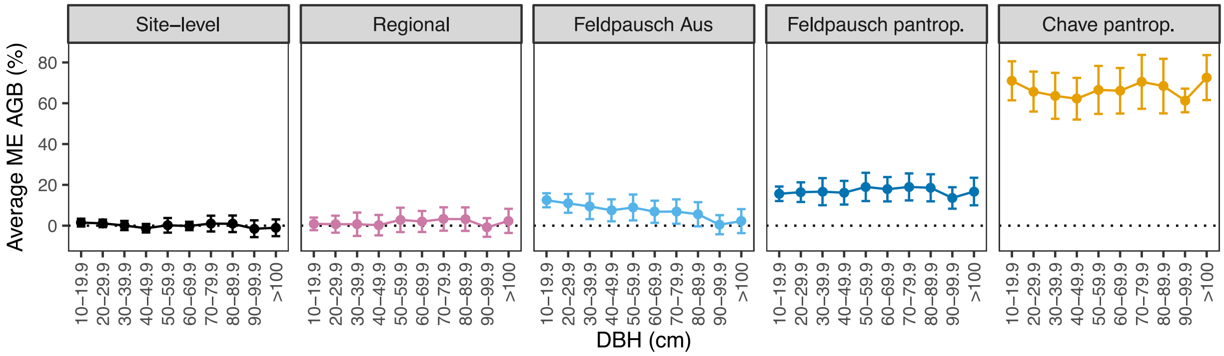

Figure 5. Size dependency of errors for aboveground biomass (AGB) derived from five *H*:DBH allometric model sets. Mean error (ME, sum of individual errors) was calculated for each 10 cm DBH size class in each plot and normalized to AGB in that sample. Points represent average ME across plots, with confidence intervals at two standard errors. Errors are shown for five model sets: site-level models derived from training data at each site (i.e. 20 models), a regional model derived from training data at all sites combined (one model, *n* = 20 sites), an Australian-region model from the literature and two pantropical models (Feldpausch et al. 2012, Chave et al. 2014). Total sample sizes for each size class were: 10–19.9 cm = 4553, 20–29.9 cm = 1325, 30–39.9 cm = 651, 40–49.9 cm = 380, 50–59.9 cm = 197, 60–69.9 cm = 105, 70–79.9 cm = 68, 80–89.9 cm = 43, 90–99.9 cm = 27, >100 cm = 35.

related to the size and representativeness of the plot (roughly 10% for a total sample size of 5 ha: (Clark and Clark 2000, Chave et al. 2004). Note that the impact of sampling uncertainties is sensitive to the number and size of plots sampled. An additional 16% random error is associated with weight measurements of AGB to construct AGB allometric equations according to traditional methodologies (Chave et al. 2004). We did not assess uncertainty caused by partial sampling of a heterogeneous landscape or uncertainties in the biomass of other life forms (Chave et al. 2004, Malhi et al. 2006), which we have not estimated here. Below, we provide further discussion of uncertainties arising from within-species wood trait variation, *H*:DBH allometric variation, and measurement errors and provide recommendations to help guide data collection under realistic scenarios.

Table 2. Accuracy (bias) and precision (variation) of five *H*:DBH allometric models derived at different biogeographic scales. Errors were calculated by comparing measured tree heights (H_{meas}) with modelled tree heights (H_{mod}). Plot-level accuracy and bias measures were based on aboveground biomass (AGB) estimates derived from H_{meas} versus H_{mod}. Accuracy measures are mean error (ME) and symmetric signed percentage bias (SSPB). Precision measures are median symmetric accuracy (MSA) and root mean squared error (RMSE). AGB error measures were normalised to plot-level AGB. Minimum and maximum errors for plots are given in square brackets.

H:DBH allometric model	Tree *H*			Plot-level AGB		Reference
	ME (m)	SSPB (%)	MSA (%)	ME (%)	RMSE (%)	
Site level	−0.1	0.2	16.7	−1.2 [−10.4, 2.5]	2.6	*This study*
Regional	0.0	1.9	17.2	1.4 [−11.6, 21.0]	7.8	*This study*
Feldpausch Aus	1.5	12.5	19.4	7.7 [−7.6, 32.5]	9.6	(Feldpausch et al. 2012)
Feldpausch pantrop.	2.3	17.2	21.5	16.9 [1.8, 39.7]	16.3	(Feldpausch et al. 2012)
Chave pantrop. (*E*)	10.5	71.0	71.1	66.6 [−25.8, 101.1]	68.3	(Chave et al. 2014)

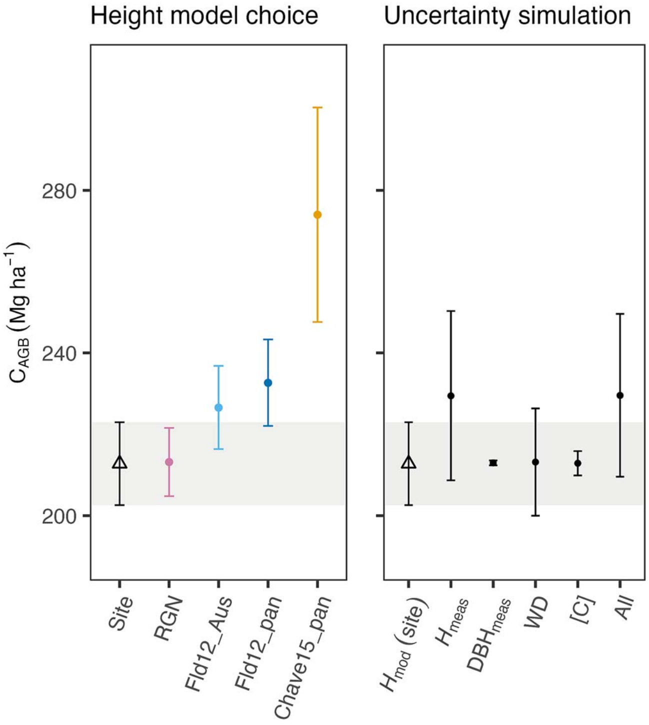

Figure 6. Carbon concentration in aboveground biomass (C_{AGB}) estimated from simulations of tree height (*H*), diameter (DBH), wood density (WD), and woody tissue carbon content [C]. Simulations were based on data for living trees in the QPRP-CSIRO network (20 sites, 7210 stems). Simulations approximate mean uncertainty in C_{AGB} arising from: (LHS) choice of *H*:DBH allometric models derived at different biogeographic scales; (RHS) other sources, including *H* measurement errors (H_{meas}), DBH measurement errors (DBH_{meas}), and within-species variation in WD and/or [C]. Plotted is mean plot-level C_{AGB} ± 2 SD (20 sites, each site first summarized as the mean of 1000 simulations), where SD is the mean of within-site standard deviations (also based on 1000 repeat simulations for each site). C_{AGB} estimated using site-level *H*:DBH models is plotted on both panels (with a triangle) ± 2 SD (shaded grey), to aid visual comparisons.

Variation in wood density and woody tissue carbon content

Though limited by sample size, our analysis indicates that species differ in their patterns of WD variation among sites and in relation to tree size. This is consistent with our expectations that species phenotypic plasticity differs and could be driven by a myriad of climate, ecological, or site characteristics in addition to phylogenetic differences (Patiño et al. 2009, Richardson et al. 2013, Martin et al. 2018). Our measured within-species WD variation (<15%, 7 species, *n* per species >9) was of similar magnitude to one prior estimate (10%, 42 species, *n* per species >6) (Chave et al. 2004) and consistent with suggestions that among-site WD variation accounts for no >20% of observed WD variation (Sungpalee et al. 2009, Siefert et al. 2015). Certain aspects of our wood sampling approach may variously lead to under- or over-estimation of WD variation. We did not sample across the full biogeographic extent of each species, for example, and we sampled the most abundant species, which may have more variable wood traits than less common, more ecologically restricted species.

Given the small uncertainty in C_{AGB} originating from within-species WD variation (1.7%), WD databases should continue to prioritise greater species-level representation, which will help reduce total error in forest carbon estimates (Phillips et al. 2019). Nonetheless, greater characterisation of within-species WD variation would be useful in advancing our capacity to predict biogeographic and age- and size-related variations in WD that influence C_{AGB}. The nature of size-related WD variation is still not well characterized, despite suggestions that the magnitude of this variation could be similar to species differences (Fortunel et al. 2020) and larger than site differences (Sungpalee et al. 2009, Siefert et al. 2015). We found that WD is lower in smaller DBH stems, consistent with some prior studies (Elias and Potvin 2003, Sungpalee et al. 2009), though Ma et al. (2020) reported WD increased with DBH. WD has also been shown to change radially through the stem and with height in the stem, in a nonsystematic manner (Plourde et al. 2014, Burt et al. 2020). In addition to mediating forest biomass at scale (Baker et al. 2004), WD variation is important to understand because it appears to be a main trait indicating drought mortality risk (O'Brien et al. 2017). More dense wood also likely has higher [C] (Elias and Potvin 2003), likely due to changes in cell wall thickness (Thomas et al. 2007, Buttò et al. 2021).

Although within-species [C] variation was greater than for WD, variation in [C] contributed less to C_{AGB} uncertainty because of the small value of the [C] coefficient. In fact, our simulations indicate a more minor influence of [C] on C_{AGB} than prior work, which suggested that better consideration of species differences in [C] could reduce the random error around C sequestration estimates by up to 10% (Elias and Potvin 2003), and could correct systematic errors by 1.6%–5.8% (Thomas and Martin 2012). Our simulations of within-species [C] variation suggest that species-level information is likely to provide sufficient accuracy and precision for forest carbon estimates.

The collation of a Global Woody Tissue Carbon Concentration Database (GLOWCAD) is already underway, with 3676 records available for 864 species (Doraisami et al. 2022). Although this extends the database assembled by Martin et al. (2018) ($n = 2228$, 636 species), both data collections still pale in comparison to the species richness of tropical forests globally and are far from being representative. Roughly one third of these data are from tropical forests, but there are no records from Australian tropical forest species and almost none from the Asian tropics. Our analysis appears to corroborate this under-sampling issue in two ways. First, despite similar mean [C] from our data as for tropical angiosperms globally (Martin et al. 2018), when we attempted to predict [C] from WD using the global regression equation in Martin et al. (2018), we systematically over-estimated [C], suggesting the equation itself is not representative of species at Australian sites. Second, the positive correlation between [C] and WD that we found at the interspecies level ($R^2 = 0.292$) was lost when species differences were accounted for using random effects. As such, we caution that equations to estimate [C] should be applied with care. We suggest that researchers prioritize the collection of new [C] data and further explore the factors that drive variation in [C] within and between species, including climate and ontogeny. Continued efforts to extend GLOW-CAD and similar databases will enable further understanding of [C] and WD variation and their effects on forest carbon uncertainties.

Height:diameter allometric model choice

Our simulations showed that overestimation of H by pantropical H:DBH models (by 17%–71%) compounded to over-estimation of mean C_{AGB} by 34.5%. Total error and bias associated with the choice of H:DBH allometric model increased from site- to regional- to pantropical models, consistent with other work (Feldpausch et al. 2012, Ledo et al. 2016, Sullivan et al. 2018, Terryn et al. 2024) and the expectation that local models better account for environmental conditions, disturbance history, and forest structure. That H and AGB bias differed substantially among plots (Table 2) further implicates the importance of allometric variation within regions, due to differences in vegetation structure, history, and climate (Table S1). We thus strongly favour development of (at least) regional-scale—rather than pantropical—allometric equations for the major continental groupings of forests in each biome.

Our findings clearly indicate that direct measures of H should be made at as many sites with appropriate stem counts as possible, either to enable the derivation of site-level H:DBH allometries or to at least ensure that diverse site-specific H:DBH relationships are represented in regional models. This might be achieved with small samples of trees (as little as 20–50, or 8% of trees in a 1 ha plots), particularly when including the largest trees, and can reduce hectare-scale uncertainty around AGB (Hunter et al. 2013, Sullivan et al. 2018). Acknowledging that resources are often limited, it may be preferable to prioritise H measurements in sites that are particularly impacted by disturbance or environmental stress. At such sites, where shorter trees are likely to dominate at a given DBH, using local H:DBH models should go a long way to reducing overestimation of regional or pantropical forest carbon (Brown et al. 1989, Chave et al. 2005).

Bias resulting from the use of pantropical H:DBH models was large and probably arises due to insufficient representation of Australian moist tropical forest in the data used to construct the models. Australian tropical forests are somewhat structurally distinct from other continents, among the most short-statured at a given DBH (Feldpausch et al. 2011) and have among the highest basal area per hectare of any tropical forests globally (Feldpausch et al. 2012, Bradford and Murphy 2019). There are, however, general inconsistencies in the biases resulting from use of pantropical models in different systems. Feldpausch et al. (2012) reported similar AGB uncertainties resulting from use of their H:DBH models as found in our study; however, Chave et al. (2014) reported much greater bias when using the Feldpausch et al. (2012) H:DBH model. In contrast, Chave et al. (2014) reported a mean AGB bias of 5.31% for their pantropical model, but the same model generated a mean plot-level AGB bias of 66.6% at QPRP-CSIRO sites. These inconsistencies might indicate different suitability of allometric equations among contexts (even for models derived from global datasets) or, to some extent, because of differences between how errors are calculated among studies. Practitioners may wish to evaluate the appropriateness of pantropical and regional H:DBH allometric equations for a given application by quantifying model errors in relation to a subset of tree H measurements for their study area.

We also note some inconsistencies in the size-dependence of errors among H:DBH models, which mirror observations that, for different forest types, H_{meas} bias can increase or decrease with H (Terryn et al. 2024). Chiefly, the regional Feldpausch et al. (2012) model tended to over-estimate H (and therefore AGB) of small trees (Fig. 5), which could result in overestimation of forest carbon at sites with more small stems. Large bias across size classes resulting from use of the Chave et al. (2014) pantropical H:DBH model is of particular concern. They may reflect prior suggestions that inclusion of climate parameters in allometric models is not universally advantageous (Hunter et al. 2013) or may reflect the shortcomings of using gridded climate data products in topographically complex regions like tropical Queensland. Biases, in particular in large size classes, can substantially shift per-hectare AGB estimates (Molto et al. 2013), since large trees contribute disproportionately to plot-level biomass (Bradford and Murphy 2019). Future work might emphasize site-level measurements of climate to better explain site-level vegetation structure and allometry. In any case, we recommend that practitioners avoid use of generic allometric equations and instead derive site-level or regional models wherever feasible.

Deployment of TLS has led to recent publication of the first pantropical H:DBH allometric equations based on TLS-derived H measurements rather than traditional inventory measurements. This work suggests that H:DBH models derived from traditional inventory methods tend to underestimate H across the range of H (Terryn et al. 2024), consistent with prior characterizations of the error distributions associated with traditional measurement techniques (Hunter et al. 2013, Larjavaara et al. 2013), which were used to account for H measurement error in our simulations here. This TLS-derived pantropical model is associated with mean uncertainty of 19.1% and mean bias of −4.8% (Terryn et al. 2024)—uncertainties of a similar magnitude to the pantropical models evaluated here. TLS clearly offers promise for rapid development of H measurement databases, which should be used to derive local-scale H:DBH allometries; however, the use of TLS-derived H measurements as inputs to AGB models derived from underestimates of H (using traditional inventory methods) may lead to over-estimation of AGB (Terryn et al. 2024). Of course, if the goal is to convert from tree volumes to biomass and carbon, LS methods also rely on prior inventory measurements and botanical identification in order to match stems with appropriate wood density values.

Height measurement error

The approximated −2.1 m downward bias for H_{meas} (Hunter et al. 2013, Larjavaara et al. 2013) scaled to an average 8.1%

under-estimation of per-hectare C_{AGB} (Table SIV). This estimate is very similar to a prior scaling of clinometer measurement errors, which resulted in an average uncertainty of 6% in plot-level biomass (Hunter et al. 2013). The real magnitude of AGB underestimation from H_{meas} bias is not well defined in our study, however, as it depends strongly on description of the H measurement error distribution. Clinometer measurements (tangent method) have variously been shown to overestimate H of tall trees, and the precision of this method is probably size-dependent, between 3% and 20% of total H (Williams et al. 1994, Hunter et al. 2013). Some authors have approximated this imprecision as 10% of total H (Chave et al. 2004), but laser rangefinder measurements (sine method) can be biased by >100% (Larjavaara et al. 2013). By way of comparison to allometric approaches, the RMSE of AGB estimates made from high-resolution, space-borne LS by Global Ecosystem Dynamics Investigation (GEDI) is 30%–40% (Dubayah et al. 2020).

Laser scanning methods provide a new scope to reduce the error associated with H measurement and AGB estimation (de Tanago et al. 2017). One group reported a 15-fold improvement in accuracy from TLS over allometric estimation of AGB (Burt et al. 2021). In addition, some work suggests that, while allometric uncertainty can increase exponentially with tree size, TLS uncertainty does not (Calders et al. 2015). Given these advantages, TLS combined with UAV-LS will very likely provide more accurate and scalable measurements of H and AGB in the coming decades (Brede et al. 2022, Terryn et al. 2022). The application of these sensor methods to AGB estimation remains limited at present, due to the still high cost of the technology and limited global availability. This need will likely be addressed in the coming years with additional support from the GEO-TREES initiative and the European Space Agency's Radar-based BIOMASS Mission (launched in 2025). Canopy climbing approaches could provide more accurate H measurements than traditional methods and help bridge the 'accuracy gap' until broader rollout of LS methods is achieved; however, the intensive resourcing required to support such an approach is widely prohibitive.

There is also scope to use statistical methods which include measurement error on the component variables of C_{AGB} to fit allometric models that better reflect these inherent uncertainties. Given the extent to which H_{meas} errors scale to C_{AGB}, it may be preferable to establish baselines of H error distributions at each study site, via repeat measurements of H by different field technicians, to enable accounting for the influence of H_{meas} errors on estimates of AGB and continued use of traditional allometric approaches. Doing so would supplement the use of LS technologies where location or resourcing do not currently support their use and support further development of LS technologies by improving the association between traditional inventory measurements and those from LS.

Conclusion

H:DBH models from the literature tended to over-estimate H and lead to highly variable C_{AGB} uncertainty among plots, whereas site-level H:DBH models minimized total error and bias for estimates of H, AGB, and C_{AGB}. Height measurement error introduced roughly 5% uncertainty to per-hectare estimates of forest carbon, which is appreciable but relatively small in comparison to the uncertainties associated with pantropical H:DBH and AGB allometric models. Within-species WD variation and [C] variation contributed <3% uncertainty to C_{AGB}; thus, efforts to database WD and [C] values should remain directed towards species-level (rather than within-species) records. Current pan-biome equations to estimate [C] from WD exhibit inconsistencies that require further development and should be applied with caution.

All existing and planned remote sensing datasets rely on field data and allometric estimates for calibration (Dubayah et al. 2020, Brede et al. 2022). While increasing use of TLS will likely reduce H and AGB measurement error, current limitations of these methods necessitate the continued development of robust allometric approaches that rely on inventory data. The pursuit to constrain uncertainties around forest carbon estimates has direct implications for detection of forest changes through time and should underpin ongoing assessments of the carbon budgets needed to limit global warming below 2°C.

Acknowledgements

We acknowledge the work of Dr Geoff Stocker to establish the QPRP plots used in this study, as well as the funding and administration support of CSIRO. We also acknowledge the CSIRO staff and many fieldwork volunteers who have maintained and censused the plots since 1971, and the many traditional owner groups who are custodians of these lands.

Author contributions

Hannah Jayne Carle (Conceptualization, Data curation, Formal analysis, Funding acquisition, Investigation, Methodology, Resources, Validation, Visualization, Writing—original draft, Writing—review & editing), Teresa Neeman (Conceptualization, Methodology, Writing—review & editing), Helen Murphy (Conceptualization, Data curation, Funding acquisition, Investigation, Resources, Writing—review & editing), David Bauman (Conceptualization, Data curation, Writing—original draft, Writing—review & editing), Oliver Binks (Investigation, Writing—review & editing), Ingrid Coughlin (Conceptualization, Investigation, Methodology, Writing—review & editing), Andrew Ford (Investigation, Resources, Writing—review & editing), Adrienne Nicotra (Funding acquisition, Investigation, Project administration, Supervision, Writing—original draft, Writing—review & editing), and Patrick Meir (Conceptualization, Investigation, Project administration, Supervision, Writing—original draft, Writing—review & editing)

Supplementary data

Supplementary data are available at *Forestry Journal* online.

Conflict of interest: None declared.

Funding

This work was supported by a seed grant funding from the Research School of Biology, The Australian National University to H.C., Australian Government Research and Training Partnership scholarship to H.C., European Union's Horizon 2020 research and innovation program under the Marie Skłodowska-Curie grant agreement no. 895799 to DB, and Catalan Science and Technology grant, Beatriu de Pinós, BP2021 00224 to OB.

Data availability

Data supporting these results can be found as cited in-text or can be released on request from Helen Murphy, CSIRO.

References

Aragão LEOC, Malhi Y, Roman-Cuesta RM. *et al.* Spatial patterns and fire response of recent amazonian droughts *Geophys Res Lett*. 2007;**34:1-5**. https://doi.org/10.1029/2006GL028946.

Baker TR, Phillips OL, Malhi Y. *et al.* Variation in wood density determines spatial patterns in amazonian forest biomass *Glob Chang Biol*. 2004;**10**:545–62.

Banin L, Feldpausch TR, Phillips OL. *et al.* What controls tropical forest architecture? Testing environmental, structural and floristic drivers *Glob Ecol Biogeogr*. 2012;**21**:1179–90.

Bauman D, Fortunel C, Delhaye G. *et al.* Tropical tree mortality has increased with rising atmospheric water stress *Nature*. 2022;**608**: 528–33. https://doi.org/10.1038/s41586-022-04737-7.

Binks O, Cernusak LA, Liddell M. *et al.* Vapour pressure deficit modulates hydraulic function and structure of tropical rainforests under nonlimiting soil water supply *New Phytol*. 2023;**240**: 1405–20. https://doi.org/10.1111/nph.19257.

Bradford M, Murphy HT. The importance of large-diameter trees in the wet tropical rainforests of Australia *PloS One*. 2019;**14**:e0208377.

Bradford MG, Murphy HT, Ford AJ. *et al.* Long-term stem inventory data from tropical rain forest plots in Australia *Ecology*. 2014;**95**:2362.

Brede B, Terryn L, Barbier N. *et al.* Non-destructive estimation of individual tree biomass: allometric models, terrestrial and uav laser scanning *Remote Sens Environ*. 2022;**280**:113180.

Brienen RJ, Phillips OL, Feldpausch TR. *et al.* Long-term decline of the amazon carbon sink *Nature*. 2015;**519**:344–8. https://doi.org/10.1038/nature14283.

Brown S, Gillespie A, Lugo A. Biomass estimation methods for tropical forests with applications to forest inventory data *For Sci*. 1989;**35**:881–902.

Burt A, Boni Vicari M, da Costa ACL. *et al.* New insights into large tropical tree mass and structure from direct harvest and terrestrial lidar *R Soc Open Sci*. 2021;**8**:201458.

Burt A, Calders K, Cuni-Sanchez A. *et al.* Assessment of bias in pantropical biomass predictions *Front For Glob Chang*. 2020;**3**:1–20. https://doi.org/10.3389/ffgc.2020.00012.

Buttò V, Rozenberg P, Deslauriers A. *et al.* Environmental and developmental factors driving xylem anatomy and microdensity in black spruce *New Phytol*. 2021;**230**:957–71. https://doi.org/10.1111/nph.17223.

Calders K, Newnham G, Burt A. *et al.* Nondestructive estimates of above-ground biomass using terrestrial laser scanning *Methods Ecol Evol*. 2014;**6**:198–208.

Chave J. *Measuring Wood Density for Tropical Forest Trees. A Field Manual for the CTFS Sites*, Vol. **6**, 2005: https://afritron.org/upload/en/manuals/wood_density_english[1].pdf.

Chave J, Andalo C, Brown S. *et al.* Tree allometry and improved estimation of carbon stocks and balance in tropical forests *Oecologia*. 2005;**145**:87–99.

Chave J, Condit R, Aguilar S. *et al.* Error propagation and scaling for tropical forest biomass estimates *Philos Trans R Soc Lond B Biol Sci*. 2004;**359**:409–20.

Chave J, Rejou-Mechain M, Burquez A. *et al.* Improved allometric models to estimate the aboveground biomass of tropical trees *Glob Chang Biol*. 2014;**20**:3177–90. https://doi.org/10.1111/gcb.12629.

Clark DB, Clark DA. Landscape-scale variation in forest structure and biomass in a tropical rainforest *For Ecol Manage*. 2000;**137**:185–98.

Condit R, Aguilar S, Hernandez A. *et al.* Tropical forest dynamics across a rainfall gradient and the impact of an el niño dry season *J Trop Ecol*. 2004;**20**:51–72.

Disney M. Terrestrial lidar: a three-dimensional revolution in how we look at trees *New Phytol*. 2019;**222**:1736–41. https://doi.org/10.1111/nph.15517.

Doraisami M, Kish R, Paroshy NJ. *et al.* A global database of woody tissue carbon concentrations *Sci Data*. 2022;**9**:284.

Dubayah R, Blair JB, Goetz S. *et al.* The global ecosystem dynamics investigation: high-resolution laser ranging of the earth's forests and topography *Sci Remote Sens*. 2020;**1**:100002.

Elias M, Potvin C. Assessing inter- and intra-specific variation in trunk carbon concentration for 32 neotropical tree species *Can J For Res*. 2003;**33**:1039–45.

Falster DS, Duursma RA, FitzJohn RG. How functional traits influence plant growth and shade tolerance across the life cycle *Proc Natl Acad Sci U S A*. 2018;**115**:E6789–98. https://doi.org/10.1073/pnas.1714044115.

Feldpausch TR, Banin L, Phillips OL. *et al.* Height-diameter allometry of tropical forest trees *Biogeosciences*. 2011;**8**:1081–106.

Feldpausch TR, Lloyd J, Lewis SL. *et al.* Tree height integrated into pantropical forest biomass estimates *Biogeosciences*. 2012;**9**: 3381–403.

Fortunel C, Stahl C, Heuret P. *et al.* Disentangling the effects of environment and ontogeny on tree functional dimensions for congeneric species in tropical forests *New Phytol*. 2020;**226**:385–95. https://doi.org/10.1111/nph.16393.

Fox J, Weisberg S. *An R Companion to Applied Regression*. 3rd edition. United States of America: SAGE Publications, Inc, 2019, 608.

Graham AW, Beech A, Bradford MG. *et al. The CSIRO Rainforest Permanent Plots of North Queensland – site, Structural, Floristic and Edaphic Descriptions*. Cairns: CSIRO and Cooperative Research Centre for Tropical Rainforest Ecology and Management, 2006.

Griscom BW, Adams J, Ellis PW. *et al.* Natural climate solutions *Proc Natl Acad Sci U S A*. 2017;**114**:11645–50. https://doi.org/10.1073/pnas.1710465114.

Hubau W, Lewis SL, Phillips OL. *et al.* Asynchronous carbon sink saturation in African and amazonian tropical forests *Nature*. 2020;**579**:80–7. https://doi.org/10.1038/s41586-020-2035-0.

Hunter MO, Keller M, Victoria D. *et al.* Tree height and tropical forest biomass estimation *Biogeosciences*. 2013;**10**:8385–99.

Hutchinson MF, Xu T, Kesteven JL. *et al. ANUClimate v2.0*, 2022. CRES, ANU, Canberra, Australia.

Ibanez T, Keppel G, Menkes C. *et al.* Globally consistent impact of tropical cyclones on the structure of tropical and subtropical forests *J Ecol*. 2018;**107**:279–92.

Jucker T, Fischer FJ, Chave J. *et al.* Tallo: a global tree allometry and crown architecture database *Glob Chang Biol*. 2022;**28**:5254–68. https://doi.org/10.1111/gcb.16302.

Keller M, Palace M, Hurtt G. Biomass estimation in the Tapajos national forest, Brazil. Examination of sampling and allometric uncertainties *For Ecol Manage*. 2001;**154**:371–82.

Kuznetsova A, Brockhoff PB, Christensen RHB. Lmertest package: tests in linear mixed effects models *J Stat Softw*. 2017;**82**:1–26.

Larjavaara M, Muller-Landau HC, Metcalf J. Measuring tree height: a quantitative comparison of two common field methods in a moist tropical forest *Methods Ecol Evol*. 2013;**4**:793–801.

Ledo A, Cornulier T, Illian JB. *et al.* Re-evaluation of individual diameter:height allometric models to improve biomass estimation of tropical trees *Ecol Appl*. 2016;**26**:2376–82.

Lines ER, Fischer FJ, Owen HJF. *et al.* The shape of trees: reimagining forest ecology in three dimensions with remote sensing *J Ecol*. 2022;**110**:1730–45.

Ma S-H, Eziz A, Tian D. *et al.* Size- and age-dependent increases in tree stem carbon concentration: implications for forest carbon stock estimations *J Plant Ecol*. 2020;**13**:233–40.

Malhi Y, Aragao LEOC, Galbraith D. *et al.* Exploring the likelihood and mechanism of a climate-change-induced dieback of the amazon rainforest *Proc Natl Acad Sci U S A*. 2009;**106**:20610–5. https://doi.org/10.1073/pnas.0804619106.

Malhi Y, Phillips OL. Tropical forests and global atmospheric change: a synthesis *Phil Trans R Soc Lond B Biol Sci*. 2004;**359**:549–55.

Malhi Y, Wood D, Baker TR. *et al.* The regional variation of aboveground live biomass in old-growth amazonian forests *Glob Chang Biol*. 2006;**12**:1107–38.

Martin AR, Doraisami M, Thomas SC. Global patterns in wood carbon concentration across the world's trees and forests *Nat Geosci*. 2018;**11**:915–20.

Molto Q, Rossi V, Blanc L. *et al.* Error propagation in biomass estimation in tropical forests *Methods Ecol Evol*. 2013;**4**:175–83.

Morley SK, Brito TV, Welling DT. Measures of model performance based on the log accuracy ratio *Space Weather*. 2018;**16**: 69–88.

Murphy GE, Romanuk TN. A meta-analysis of declines in local species richness from human disturbances *Ecol Evol*. 2014;**4**: 91–103. https://doi.org/10.1002/ece3.909.

O'Brien M, Engelbrecht B, Joswig J. *et al.* A synthesis of tree functional traits related to drought-induced mortality in forests across climatic zones *J Appl Ecol*. 2017;**54**:1669–86.

Pan Y, Birdsey RA, Fang J. *et al.* A large and persistent carbon sink in world's forests *Science*. 2011;**333**:988–93. https://doi.org/10.1126/science.1201609.

Pan Y, Birdsey RA, Phillips OL. *et al.* The enduring world forest carbon sink *Nature*. 2024;**631**:563–9. https://doi.org/10.1038/s41586-024-07602-x.

Patiño S, Lloyd J, Paiva R. *et al.* Branch xylem density variations across the amazon basin *Biogeosciences*. 2009;**6**:545–68.

Phillips OL, Brienen RJW, RAINFOR collaboration. Carbon uptake by mature amazon forests has mitigated amazon nations' carbon emissions *Carbon Balance Manag*. 2017;**12**:1.

Phillips OL, Sullivan MJP, Baker TR. *et al.* Species matter: Wood density influences tropical forest biomass at multiple scales *Surv Geophys*. 2019;**40**:913–35. https://doi.org/10.1007/s10712-019-09540-0.

Plourde BT, Boukili VK, Chazdon RL. *et al.* Radial changes in wood specific gravity of tropical trees: inter- and intraspecific variation during secondary succession *Funct Ecol*. 2014;**29**:111–20.

R Core Team. *R: A Language and Environment for Statistical Computing*. Vienna, Austria: R Foundation for Statistical Computing, 2025.

Richardson SJ, Allen RB, Buxton RP. *et al.* Intraspecific relationships among wood density, leaf structural traits and environment in four co-occurring species of nothofagus in New Zealand *PloS One*. 2013;**8**:e58878.

Rodriguez-Zaccaro FD, Valdovinos-Ayala J, Percolla MI. *et al.* Wood structure and function change with maturity: age of the vascular cambium is associated with xylem changes in current-year growth *Plant Cell Environ*. 2019;**42**:1816–31. https://doi.org/10.1111/pce.13528.

Roxburgh SH, Paul KI, Clifford D. *et al.* Guidelines for constructing allometric models for the prediction of woody biomass: how many individuals to harvest? *Ecosphere*. 2015;**6**:1–27.

Siefert A, Violle C, Chalmandrier L. *et al.* A global meta-analysis of the relative extent of intraspecific trait variation in plant communities *Ecol Lett*. 2015;**18**:1406–19. https://doi.org/10.1111/ele.12508.

Sullivan MJP, Lewis SL, Hubau W. *et al.* Field methods for sampling tree height for tropical forest biomass estimation *Methods Ecol Evol*. 2018;**9**:1179–89. https://doi.org/10.1111/2041-210X.12962.

Sungpalee W, Itoh A, Kanzaki M. *et al.* Intra- and interspecific variation in wood density and fine-scale spatial distribution of stand-level wood density in a northern Thai tropical montane forest *J Tropical Ecol*. 2009;**25**:359–70.

de Tanago JG, Lau A, Bartholomeus H. *et al.* Estimation of above-ground biomass of large tropical trees with terrestrial lidar *Methods Ecol Evol*. 2017;**9**:223–34.

Terryn L, Calders K, Bartholomeus H. *et al.* Quantifying tropical forest structure through terrestrial and uav laser scanning fusion in Australian rainforests *Remote Sens Environ*. 2022;**271**:112912.

Terryn L, Calders K, Meunier F. *et al.* New tree height allometries derived from terrestrial laser scanning reveal substantial discrepancies with forest inventory methods in tropical rainforests *Glob Chang Biol*. 2024;**30**:e17473.

Thomas DS, Montagu KD, Conroy JP. Temperature effects on wood anatomy, wood density, photosynthesis and biomass partitioning of eucalyptus grandis seedlings *Tree Phys*. 2007;**27**:251–60.

Thomas SC, Martin AR. Carbon content of tree tissues: a synthesis *Forests*. 2012;**3**:332–52.

Walker WS, Gorelik SR, Cook-Patton SC. *et al.* The global potential for increased storage of carbon on land *Proc Natl Acad Sci U S A*. 2022;**119**:e2111312119.

Williams M, Bechtold W, LaBau V. Five instruments for measuring tree height: an evaluation *South J Appl For*. 1994;**18**:76–82.

Forestry: An International Journal of Forest Research, 2025, **00**, 1–12
https://doi.org/10.1093/forestry/cpaf084
Original Article